Extended Abstracts of the 2003 International Conference on Solid State Devices and Materials, Tokyo, 2003, pp. 432-433

P2-11

Characterization and Modeling of High Q-Factor, High Resonant Frequency Spiral Inductors with 6 μm thick Top-Metal for RF-IC Applications

Yo-Sheng Lin, Hong-Wei Chiu[+], Shen-Hong Wu, and Shey-Shi Lu[+], *Senior Member, IEEE*

Department of Electrical Engineering, National Chi-Nan University, Puli, Taiwan, R.O.C.
Phone: 886-4-92910960 ext.4101, Fax: 886-4-92917810, Email : stephenlin@ncnu.edu.tw
[+]Department of Electrical Engineering, National Taiwan University, Taipei, Taiwan, R.O.C.

Summary

In this paper, we demonstrate a comprehensive analysis of the effects of the layout, temperature (from -50°C to 200°C), top metal thickness, and substrate resistance on the performances of high quality-factor (Q-factor) and high resonant frequency (f_{SR}) spiral inductors with 6 μm thick top metal in deep sub-micron CMOS technology for radio-frequency integrated circuit (RF-IC) applications for the first time [1]-[3]. Metal width, metal space, and inner dimension were carefully selected to optimize Q-factor and f_{SR} based on simulated results of EM simulation tool SONNET. We found that Q-factor decreases with increasing temperature but shows a reverse behavior at a higher frequency range. In addition, the reverse frequency f_R, which corresponds to zero temperature coefficient of Q-factor, increases with increasing substrate resistance. This phenomenon can be explained by the positive temperature coefficients of the metal series resistance (R_s) and the substrate resistance (R_{sub}). The above results will facilitate RF designers to catch the temperature behavior of the on-chip spiral inductors.

Table I is a summary of the key layout parameters and extracted small-signal equivalent circuit parameters at room temperature (25°C) of the inductors under study. All the inductors have the same inner dimension, metal width, and metal space. The only difference is the turn number for the convenience of performance comparison. As can be seen, low metal series resistance is achieved mainly due to the 6 μm thick top metal. In addition, the extracted inductance, ranging from 0.9 nH to 13.93 nH are wide enough for RF-IC design. Fig. I shows the small-signal equivalent circuit model of the inductors under study, which includes the extrinsic pads. Extrinsic open pad models at various temperatures were extracted based on the fitting of the simulated and measured S-parameters of the open pad structure under various temperatures. Fig. 2 (a) shows the measured and simulated Q-factor versus frequency characteristics of inductor-B. The extrinsic pads have much effect on the performance of inductors. As can be seen, the maximum Q-factor (Q_{max}) and f_{SR} of the intrinsic part of inductor-B is 23.6 and 19.5 GHz, respectively, while the Q_{max} and f_{SR} of inductor-B includes the extrinsic pads is 21 and 17 GHz, respectively. Fig. 2(b) shows the measured and simulated S-parameters of inductor-B. Fig. 2(c) shows the measured and simulated inductance versus frequency characteristics of inductors B and E. As can be seen, the simulated results conform to the measured data. Fig. 3 (a) shows the measured Q-factor versus frequency characteristics of inductors A, B, C, and E. Fig. 3(b) shows the measured and simulated Q-factors versus frequencies characteristics of inductors with the layout of inductor-B but with various different top metals.

All the inductors were measured at various temperatures (-50, -25, 0, 25, 75, 125 and 200°C) to study the temperature effect on the performances of inductors with various top metals, layouts, and substrate resistances. Table II is a summary of the extracted small-signal equivalent circuit parameters of inductor-B at several key temperatures. Fig. 4 shows the measured Q-factor versus frequency characteristics of inductor-B at various temperatures. We found that Q-factor decreases with increasing temperature but it shows a reverse behavior at a higher frequency range. In addition, the reverse frequency f_R, which corresponds to zero temperature coefficient of Q-factor, increases with increasing substrate resistance. Table III is a summary of the extracted small-signal equivalent circuit parameters of inductor-B before and after proton bombardment. Fig. 5 shows the Q-factors versus frequency characteristics of inductor-B before and after proton bombardment. The proton bombardment process increases the Q_{max} from 23.6 to 48.7, which is mainly due to the increase of substrate resistance. We also found that the transmission line loss and coupling loss between devices can be largely decreased after proton bombardment. This means this post process is very promising for high performance RF-ICs.

References

[1] J. M. L. Villegas et al., *IEEE Trans. on Microwave Theory Tech*., vol. 48, pp. 76-83, Jan. 2000.
[2] A. Zolfaghari, *IEEE J. Solid-State Circuits*, vol. 36, pp. 620-628, April 2001.
[3] C. C. Tang et al., *IEEE J. Solid-State Circuits*, vol. 37, pp. 471-480, no. 4, Apr. 2002.
[4] Rob Groves et al., IEEE J. Solid State Circuits, vol. 32, no. 9, pp. 1455-1459, 1997.
[5] G. M. Stojanovic et al., *IEEE Proc. 22nd International Conference on Microelectronics*, Serbia, pp. 469-472, 2000.

Table I Key layout parameters and extracted small-signal equivalent circuit parameters of the inductors.

Inductor No.	A	B	C	D	E	F	G
W (μm)	11						
S (μm)	5						
Top Metal (μm)	6						
Inner Dimension (μm×μm)	137.5×137.5						
T (°C)	25						
Turn Number	1.5	2.5	3.5	4.5	5.5	6.5	7.5
L_s (nH)	0.90	1.99	3.90	6.83	8.57	11.49	13.93
R_s (Ω)	0.50	1.20	2.10	3.00	3.49	4.29	6.02
C_s (fF)	19.76	12.51	16.27	19.50	23.92	26.23	30.43
C_{ox1} (fF)	56.8	52.7	59.7	67.7	84.4	102.0	136.9
C_{ox2} (fF)	54.9	50.4	54.3	64.1	77.2	100.0	135.6
C_{sub1} (fF)	25.0	38.5	52.1	68.4	80.2	88.3	93.8
C_{sub2} (fF)	25.0	38.5	52.1	68.4	79.7	86.0	88.8
R_{sub1} (Ω)	510.0	736.6	703.5	671.2	490.9	371.2	318.8
R_{sub2} (Ω)	500.0	736.6	703.5	671.2	488.6	369.3	317.7

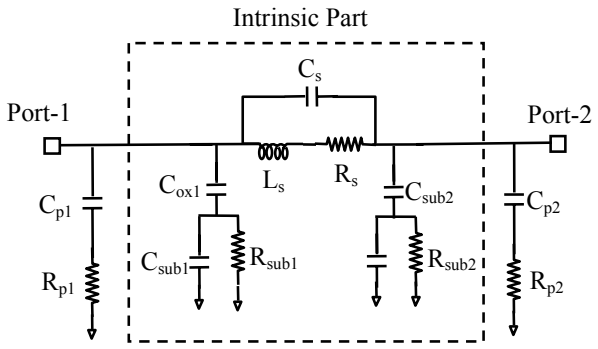

Fig. I Small-signal equivalent circuit model (including the extrinsic pads) of the inductors under study.

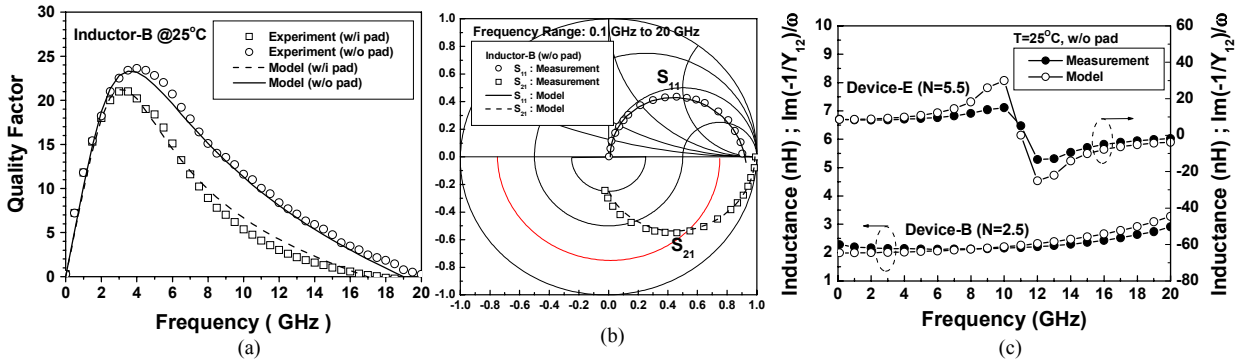

(a) (b) (c)

Fig. 2 (a) Measured and simulated Q-factor versus frequency characteristics of inductor-B. (b) Measured and simulated S-parameters of inductor-B. (c) Measured and simulated inductance versus frequency characteristics of inductors B and E.

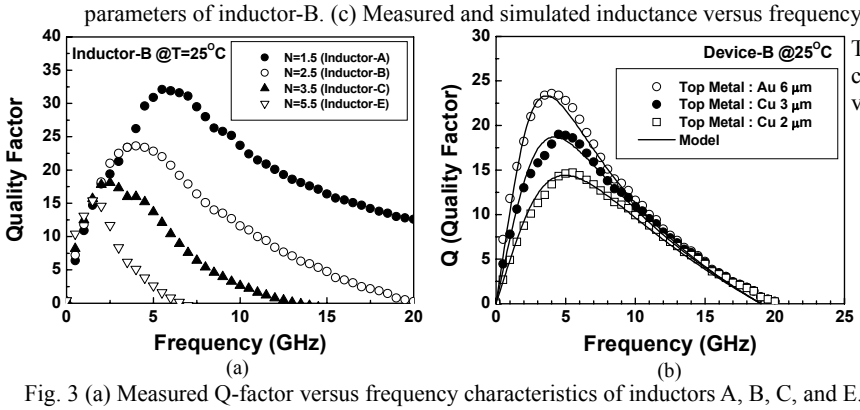

(a) (b)

Fig. 3 (a) Measured Q-factor versus frequency characteristics of inductors A, B, C, and E. (b) Measured and simulated Q-factors versus frequencies characteristics of inductors with the layout of inductor-B but with various top metals.

Table II Extracted small-signal equivalent circuit parameters of inductor-B at various key temperatures.

Inductor No.	B			
W (μm)	11			
S (μm)	5			
Top Metal (μm)	6			
Inner Dimension (μm×μm)	137.5×137.5			
Turn Number	2.5			
T (°C)	-25	0	25	200
Substrate Thickness (μm)	750			
L_s (nH)	1.94	1.94	1.99	2.39
R_s (Ω)	0.90	0.93	1.20	2.77
C_s (fF)	12.51	12.51	12.51	6.59
C_{ox1} (fF)	54.0	52.7	52.7	52.7
C_{ox2} (fF)	51.6	50.4	50.4	50.4
C_{sub1} (fF)	63.8	50.0	38.5	27.0
C_{sub2} (fF)	64.9	50.4	38.5	26.7
R_{sub1} (Ω)	588.2	662.4	736.6	1256
R_{sub2} (Ω)	587.0	661.8	736.6	1260

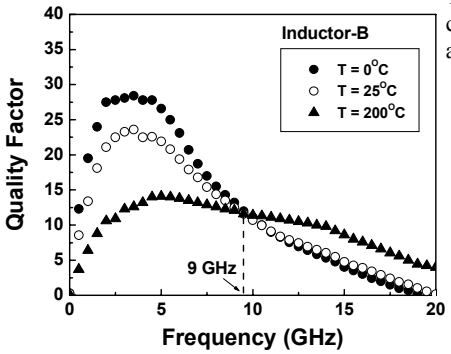

Fig. 4 Measured Q-factor versus frequency characteristics of inductor-B under various temperatures.

Table III Extracted small-signal equivalent circuit parameters of inductor-B before and after proton bombardment.

Inductor No.	B	
W (μm)	11	
S (μm)	5	
Top Metal (μm)	6	
Inner Dimension (μm×μm)	137.5×137.5	
Turn Number	2.5	
T (°C)	25	
Proton Bombardment	No	Yes
L_s (nH)	1.99	1.99
R_s (Ω)	1.20	1.20
C_s (fF)	12.51	12.51
C_{ox1} (fF)	52.7	52.7
C_{ox2} (fF)	50.4	50.4
C_{sub1} (fF)	38.5	34.2
C_{sub2} (fF)	38.5	34.2
R_{sub1} (Ω)	736.6	7316.3
R_{sub2} (Ω)	736.6	7316.3

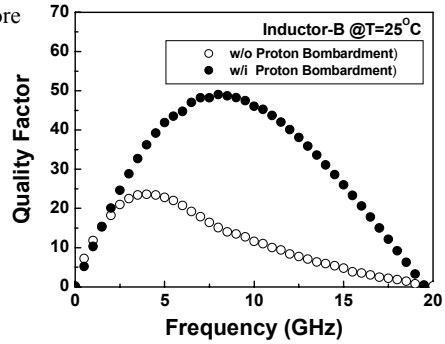

Fig. 5 Quality factors versus frequency characteristics of inductor-B before and after proton bombardment.